ACS APPLIED MATERIALS & INTERFACES

Research Article

www.acsami.org

Versatile Microfluidic Droplets Array for Bioanalysis

Shan-Wen Hu, Bi-Yi Xu, Wei-ke Ye, Xing-Hua Xia, Hong-Yuan Chen, and Jing-Juan Xu*

State Key Laboratory of Analytical Chemistry for Life Science, School of Chemistry and Chemical Engineering, Nanjing University, Nanjing 210093, P.R. China

Supporting Information

ABSTRACT: We propose a novel method to obtain versatile droplets arrays on a regional hydrophilic chip that is fabricated by PDMS soft lithography and regional plasma treatment. It enables rapid liquid dispensation and droplets array formation just making the chip surface in contact with solution. By combining this chip with a special Christmas Tree structure, the droplets array with concentrations in gradient is generated. It possesses the greatly improved performance of convenience and versatility in bioscreening and biosensing. For example, high throughput condition screening of toxic tests of CdSe quantum dots on HL-60 cells are conducted and cell death rates are successfully counted quickly and efficiently. Furthermore, a rapid biosensing approach for cancer biomarkers carcinoma embryonic antigen (CEA) is developed via magnetic beads (MBs)-based sandwich immunoassay methods.

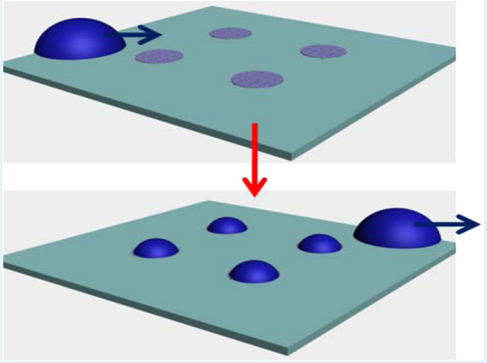

KEYWORDS: *droplets array, liquid dispensation, surface wettability, rapid analysis*

INTRODUCTION

Microfluidic devices are showing significant potential in biological processing and chemical reactions, offering many advantages, such as miniaturization, automation, and low reagents consumption, and becoming attractive candidates for next-generation biosensors and bioscreening devices.[1,2] In traditional methods, it is laborious and time-consuming that samples need to be sent to laboratory for accurate equipment analysis.[3−5] To overcome these shortcomings, microfluidics-based biochips provide a convenient way for analysis. Thus, there is a strong need for an ideal analysis chip that should be assured to be affordable, sensitive, specific, user-friendly, rapid, robust, equipment-free, and deliverable to the end-user.[6]

For a user-friendly microfluidic device, one of the challenging operations is the efficient liquid dispensation, since bio-reactions are often performed in a small volume ranging from nanoliters to microliters. Traditional analysis methods need accurate pipettors thay are not common commodities for end-users. So, it is urgent to develop a simple and practical manner to transfer and disperse liquid precisely and quantitatively. Recently, a lot of effort has been made to achieve this goal.[7] Liquid-jet printing[8−10] and the ultrasonic droplets generation technique[11,12] are used to transfer liquid accurately on various substrates in the range of picoliters.[13] Pump on chip often utilizes mechanical forces such as pressure and centrifuge to disperse samples continuously.[14] On the other hand, flow-through techniques based on surface free energies build a surface modified chip to guide liquid without extra force.[15−18] Toma and coauthors have previously reported an excellent work involving coating AuNPs on a Teflon nanocone array surface for droplets dispensing after being spotted by droplets of polydopamine.[19] Furthermore, array detection is a promising way to improve the throughput.[20−22] However, macro arrays such as a 96-well plate require numerous pipetting operations. Wang et al. proposed a microwell array to handle liquid dispensation in nanoliter range and realize PCR reactions without cross-contamination.[23] However, it is worth noting that these techniques all rely on well-trained people; a more convenient and versatile chip with better performance is anticipated to be exploited for combinatorial synthesis, cell-based analysis, and screenings.

Herein, we proposed a microfluidic device with a novel way for liquid dispensation without complicated control system or extra forces. We built a regional hydrophilic chip via plasma treated PDMS with nanopatterns. Just contacting the chip surface with the reagent, a droplets array was obtained automatically, which made the chip an ideal platform for diagnostic testing. Droplets from picoliters to nanoliters were obtained. By combining this chip with a Christmas Tree gradient generator, a droplet array in gradient was achieved, showing its superiority in integration. A rapid biosensing chip for carcinoma embryonic antigen (CEA) was developed via labeled magnetic beads (MBs). This chip meets the requirement of being user-friendly and may be developed as a new tool for the point-of-care analysis.

EXPERIMENTAL SECTION

Materials. Polydimethylsiloxane (PDMS) materials including Sylgard 184 elastomer base and curing agent were both purchased from Dow Corning (Midland, MI). Ethidium bromide (EB) was

Received: October 29, 2014
Accepted: December 19, 2014
Published: December 19, 2014

DOI: 10.1021/am5075216
ACS Appl. Mater. Interfaces 2015, 7, 935−940

purchased from Sigma. Methylene blue was provided by Shanghai Reagent Co, Ltd. Phosphate buffered saline (PBS; 10 mM) and 50 mM MES buffer were purchased from Shenggong Co, Ltd. Acute myeloblastic leukemia (HL-60) cells were cultured and propagated in DMEM cell culture medium (Gibco) with 10% fetal bovine serum and 100 mg L^{-1} penicillin and 100 mg L^{-1} streptomycin at 37 °C under 5% CO_2 in standard incubator.

Microfluidic Chip Fabrication. Experimentally, we first built the nanostructure on a Si substrate. Briefly, a ⟨100⟩ p-type silicon wafer was patterned with a layer of 500 nm thick positive photoresisitor to form an array of round pads by traditional photolithography. Then, the wafer was subject to 5 nm gold deposition by physical vapor deposition (PVD). After that, the whole wafer was subject to reactive ion etching (RIE) to generate the regional rough pads. After washing the photoresistor away, the silicon wafer with patterned rough pads was ready as a mold. As shown in Figure 1a–c, we transferred this

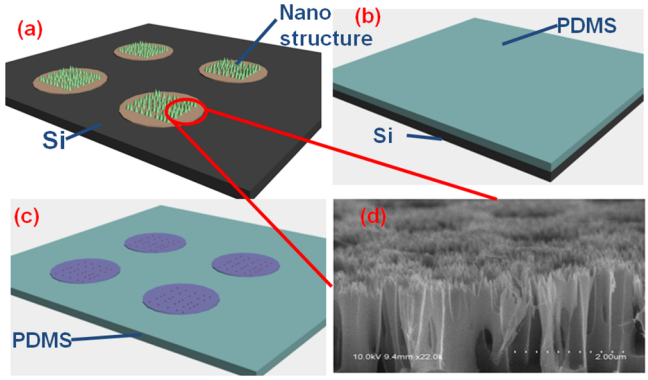

Figure 1. Diagram of the chip making process. (a) Microstructure on silicon substrate; (b) PDMS soft lithography process; (c) PDMS chip with sampling zone; (d) SEM image of the micro- and nanostructure on silicon substrate.

pattern to PDMS chip via PDMS soft lithography. PDMS monomer and the curing agent were thoroughly mixed at the ratio of 10:1, poured on Si mold, cured at 80 °C for 90 min, and then peeled off. Then, the chip was treated with oxygen plasma with a mask covering the surface outside the nanopattern area. Due to the fact that the effect of plasma treatment on PDMS decayed quickly, chitosan was used to modify the surface. Chitosan was dissolved in 3% acetic acid solution at the ratio of 0.01% (m/v). We dipped our PDMS chip into chitosan solution and lifted it up to get a chitosan droplets array. Then, the chip was incubated for 2 h at room temperature, and the chitosan droplets were washed out.

Droplets Array in Concentration Gradient. For droplets in gradient, this chip (layer B) was combined with a Christmas Tree gradient generator (layer A). The PDMS layer A was fabricated from a glass mold made via typical microlithography methods.[24] Then, layer A was treated by plasma and stored for 1 h before it covered layer B. For dye solution visualization analysis, pure water was injected from the inlet A and Methylene blue was injected from inlet B. After the gradient was generated and became stable in the channels, the top layer was peeled off and the sampling chip was lifted up to generate droplets.

CdSe quantum dots were synthesized by the following methods.[25] Briefly, 15.13 mg Na_2SO_3 was dissolved in 50 mL dd water, adding 4.74 mg Se while stirring. The mixture was refluxed gently with stirring for 2 h as solution A. Then, 54.80 mg $CdCl_2{\cdot}2.5H_2O$ was dissolved in 10 mL water with 52 μL MPA, and the pH was adjusted to 9 by 1 M MPA as solution B. The two solutions were mixed and refluxed with stirring for 6 h.

CdSe quantum qots in solution was injected from inlet B to generate a gradient array with water from inlet A. After desiccation, this chip was used to capture droplets of cells in solution. Cultured at 37 °C for 24 h, cells were stained by 100 μg/mL EB. The resulting images were captured by the Leica DMIRE2 microscope fluorescence analyzing system. Cell death rate data were collected by Image-Pro Plus (IPP) program.

Rapid Biosensing for CEA. Antibodies for CEA conjugated MBs (Ab-MBs) were acquired following the typical methods.[26] First, 100 μL 10 mg/mL MBs with carboxyl groups were thoroughly washed by MES buffer. Then, 200 μL EDC/NHS (40 mg·mL^{-1}/20 mg·mL^{-1}) was used to activate carboxyl groups on MBs for 1 h at room temperature. Afterward, MBs were washed thoroughly by PBS. Second, 150 μL 1.0 mg/mL Ab was added into the activated MBs and incubated 12 h at room temperature with rotation. At last, the Ab-MBs were washed and kept at 4 °C in 500 μL PBS, which contains 1% BSA (w/v) and 0.05% NaN_3.

Ab-MBs were diluted 100 times before being used to for biosensing. Droplets of diluted Ab-MBs were captured on chip via process shown in Figure 2b. Then magnetic field was applied. Target CEA antigens at

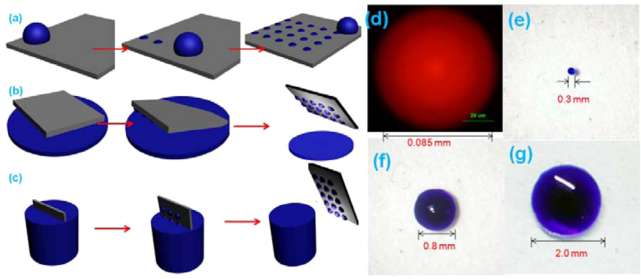

Figure 2. (a–c) Diagram of the droplets generating process. (d) Microscope image of a droplets at 85 μm (Rhodamine B). (e–g) Camera images of droplets (methylene blue) in different sizes.

different concentrations were added on chip following the same sampling method. After incubating for 1 h, the chip was washed with PBS three times and the HRP-conjugated CEA antibody was added on the chip. After the incubation and washing, 3,5,3′,5′-tetramethylbenzidine (TMB) was added and absorbance intensity data were collected via a Thermo Scientific Varioskan Flash (Thermo Fisher Scientific, U.S.A.).

RESULTS AND DISCUSSION

Characterization of Surfaces. The roughness of the surface had significant effect with the wettability, so we utilized a nanopattern to improve the roughness of the surface so as to change the wettability.[27] First on silicon template, as shown in Figure 1d, columns were built on silicon substrate in an array, the height can be as high as 2 μm with needles in nanoscale on top. Hence, the surface roughness was improved; textured surface helped to promote superwetting behavior.[28−30] The surface wettability of silicon substrate was changed greatly due to a higher specific surface area. The contact angle changed from 72.8° to 23.1°.

In order to improve the reproducibility and reduce the cost, we transferred this pattern to PDMS via PDMS soft lithography. The columns and needles improved the surface roughness. The contact angle of bare PDMS surface was 108.3°, and it changed to 119.4° with pattern.

Plasma treatment can turn the hydrophobic surface of PDMS into a hydrophilic surface. After the same treatment, PDMS with pattern and without pattern showed a difference in hydrophilicity. The contact angle of bare PDMS changed to 24.6° while patterned PDMS changed to near 0°, showing that higher roughness enhanced the hydrophilicity and helped improve the wettability. To make the surface permanently hydrophilic, we applied surface modification to dress the rough surface with stable hydroxyl groups via chitosan. The recovery

DOI: 10.1021/am5075216
ACS Appl. Mater. Interfaces 2015, 7, 935−940

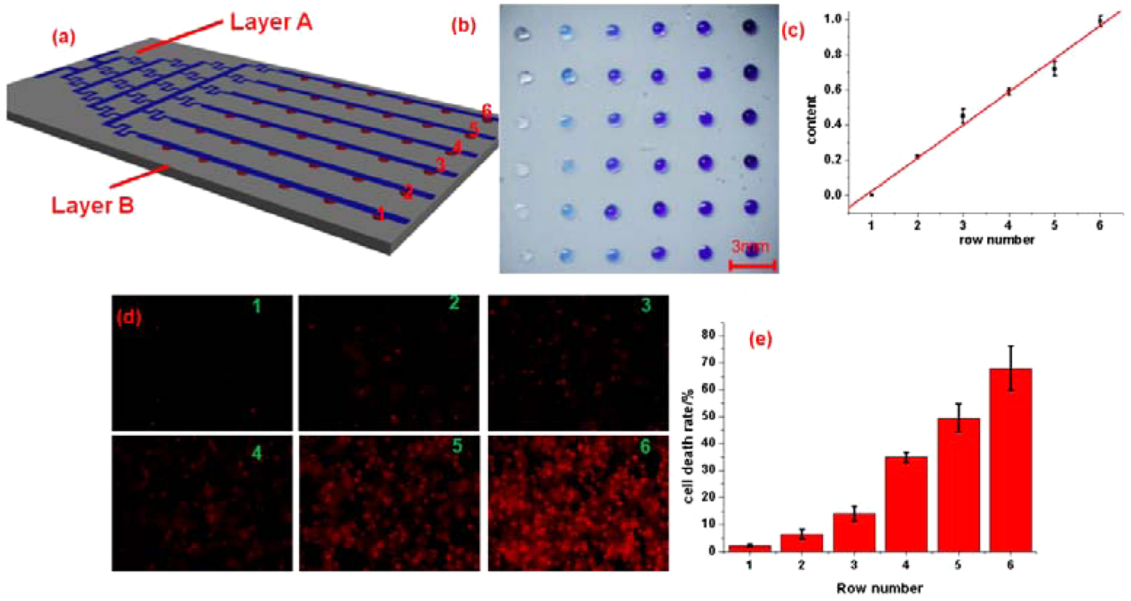

Figure 3. (a) Diagram of the combination of the gradient generator and the sampling chip. (b) MB droplets in a gradient array. (c) Dye solution visualization analysis results of the droplets gradient. (d and e) Toxicity screening of CdSe on HL-60 cells: (d) EB staining images; (e) death rates statistical results.

curve of bare PDMS and chitosan modified PDMS after plasma treatment was shown in Supporting Information (Figure S1b). The contact angle of bare PDMS increased faster and larger. Chitosan modified chip reached steady state (52°) earlier and showed more hydrophilic at the steady state.[31] This difference was amplified when it comes to PDMS with nanostructure.

Characterization of Droplets Array. This regional hydrophilic chip showed a peculiar characteristic. If we dip it into water and lift it up, water will rapidly slide down in the hydrophobic regions due to the lotus effect,[32] while in the hydrophilic area it remains stuck on the surface. On this device, as long as droplets form on hydrophilic regions, they will spread to the boundary of the hydrophobic regions, which helps to balance the gravity of the droplets, so that even if the chip is vertically lifted up from the sample, droplets will not slide down. Hence, we utilize this phenomenon for fast sampling in bioanalysis. As shown in Figure 2, we can achieve this array by adding a large droplet on the chip and waving the chip to let the droplet run through the whole chip (a), making the chip glance at a solution layer (b), or dipping the chip into solution if the volume is huge (c). Throughout the process, the chip is placed in an environment with saturated vapor to prevent water evaporation.

To determine the height of the droplet experimentally, a series of dots with different heights was filled with FITC (10 μM), and the fluorescence intensity was determined. The fluorescence intensity (FI) was found to have a linear relationship with the height. Hence, a working curve was made; then, a droplets array of FITC (10 μM) was captured; the FI was determined to detect the height.

The liquid volume of droplets was controlled by the size of the hydrophilic region. We developed this automatic sampling method to satisfy sampling needs at different ranges. By controlling the bottom area, we were able to capture different droplets ranging from 500 pL to 700 nL. Droplets of methylene blue were captured. At the diameter of 2000 μm, the average height was 422 μm (deviation = 10.4 μm, coefficient of variation (CV) = 0.025); the volume was about 700 nL. With the diameter of 300 μm, the average height was 62 μm (deviation = 15.2 μm, CV = 0.24), leading to a volume of 2 nL. The lower limit of volume was determined by the alignment process. When the droplets get smaller, it is harder to align and the error of alignment cannot be neglected. Camera images of droplets in different sizes are shown in Figure 2e–g. The smallest droplets we captured were 500 pL, with diameter of 85 μm, and the microscope image is shown in Figure 2d. When the diameter was 800 μm, the average height was 201 μm with a standard deviation of 11.3 μm (CV = 0.056); hence, the volume was ca. 54 nL. We captured a 6 × 6 droplets array of water (d = 800 μm); the whole mass was 1.86 mg. Given ρ = 0.999126 g/cm^3, we obtain the average volume of the droplets of 51.7 nL, which is similar to the result of fluorescence method.

A mask was needed during the plasma treatment to cover the surface outside the nanopattern area. The distance between the mask and the PDMS substrate was found to have a significant effect on the uniformity of droplets array. The mask should be thin enough and firmly pressed to the substrate. Regional modification by chemical is equivalent to an ideally bonded mask, which will improve the uniformity of the droplets.

Droplets Array in Concentration Gradient. Compared with the size of diameter, the depth of the sensing area could be ignored. This made the platform easier to integrate with other microfluidic units. We combined the sampling chip with a gradient generator; a droplets array with droplets in different concentrations was obtained. Methylene blue solution and water were mixed in the Christmas Tree structure and ran to the main liquid channels at different ratios. Solutions ran along and filled both the hydrophilic area and hydrophobic area. As with our previous work,[33] each channel has different proportion of water from inlet A and methylene blue from inlet B, the color changed from transparent to blue, confirming the gradient was generated. After the top layer was peeled off, we lifted the bottom layer up to get the droplets array. Since the sampling zones contacted with different channels, the captured droplets (d = 800 μm) were the same concentration as the liquid in channels, making this array in gradient. The concentrations of

DOI: 10.1021/am5075216
ACS Appl. Mater. Interfaces 2015, 7, 935–940

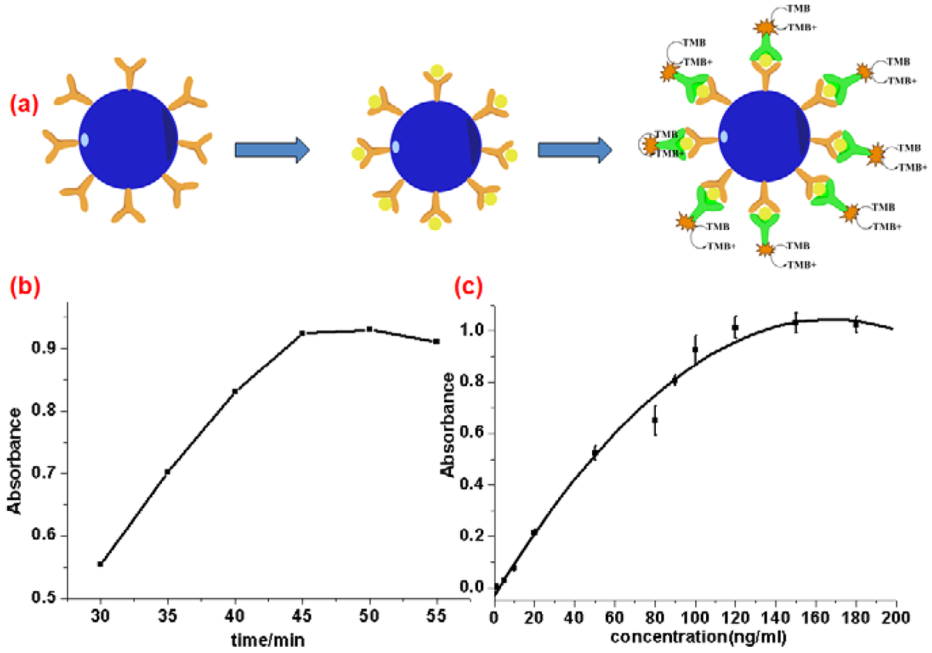

Figure 4. (a) Diagram of the detection process of CEA by MB probes. (b) The incubation time for biorecognition between CEA and capture antibody immobilized on MBs. (c) Calibration curve of the biosensing approach for CEA detection (n = 4).

droplets are characterized by the dye solution visualization analysis.[33] As shown in Figure 3b, droplets are in a clear gradient. Colors of methylene blue and water mixing at different ratios were determined to get a working curve. Characteristic results in Figure 3c showed this gradient is in good linearity.

As a model application, toxicity screening of CdSe quantum dots on chip was executed in a 6 × 6 droplets array. Toxicity screening of quantum dots was necessary to evaluate its quality. The procedure is usually laborious and time-consuming. It includes numerous pipetting actions to transfer, disperse, and mix, which adds to its complexity and uncertainty. In this work, these steps could be automated on our chip, which greatly improved the work efficiency. The gradient of quantum dots was characterized by its FI, as shown in Supporting Information Figure S2a, while its ability of entering cells was confirmed by Figure S2b. Six concentrations of CdSe were tested at one time with six repeats—less handwork lead to higher consistency. As shown in Figure 3d, cells showed a decrease in viability as concentration of CdSe increases.

Rapid Biosensing to CEA. The principle of this sandwich immunoassay process is shown in Figure 4a. The whole ELISA process could be done within 2 h. The unique sampling method reduced the workload further. CEA was chosen as analyte. Carboxylated MBs were bound with primary antibody via amido bond. Then, CEA was captured by the immobilized antibody; specifically, the antibody for CEA with HRP functionalized was used as a detective marker for TMB-based colorimetric detection.

We utilized MBs for immobilization of capturing antibodies. To confirm the immobilization, the Dynamic Light Scattering (DLS) was used to measure the size distribution of MBs before and after the immobilization. As shown in Supporting Information Figure S3, the mean diameter of MBs is 941.0 nm. After antibody immobilization, it changed to 992.0 nm. Droplets of Ab-MBs were captured on chip, and MBs can be immobilized on the surface if magnetic field is applied. This makes the chip washable and reusable. FITC-BSA conjugated MB was used to evaluate the loss during washes. With magnetic field applied, FI reduced less than 10% after five washes. Without magnetic field applied, reagents can be totally washed out.

The signal was found to be dependent on the concentration of the Ab-MBs probe. We utilized 100 ng/mL CEA for optimization assays. The absorbance value increased as the concentration of Ab-MBs increased and reached a plateau at 10 μg/mL. However, the noise signal also increased, since nonspecific bonding on probes increased. Therefore, 10 μg/mg was chosen as an optimized condition.

The absorbance intensity also increased with the incubation time for biorecognition between CEA and Ab-MBs, and it reached a plateau at 45 min (Figure 4b). The time is shorter than ELISA on plate, because droplets on chip provided a shorter diffusion distance from immobilized antibodies to antigens,[34,35] which improved work efficiency further.

The adsorption of protein on hydrophobic surface is mainly determined by the concentration of protein and contact time. Herein, during the liquid dispensation process, the hydrophobic surface makes contact with the protein solution in a very short time, which could reduce the chance of protein adsorption. On the other hand, the highest concentration of protein solutions we used in biosensing assays is 10 μg/mL. We can dip the chip in samples 10 times without losing the ability of capturing droplets. However, if the concentrations are above 10 mg/mL, the chip will lose the ability of capturing droplets due to protein surface adsorption.

Absorbance intensity was found to have a linear relationship with CEA concentration at range from 10 to 100 ng/mL, while the limit of detection was 5 ng/mL (Figure 4c). Therefore, a biosensing chip for fast detection of CEA was developed. The linear range and limit of detection was typically based on the HRP-TMB sandwich immunoassay methods; higher sensitivity can be achieved by coupling amplification mechanism in future work.

DOI: 10.1021/am5075216
ACS Appl. Mater. Interfaces 2015, 7, 935−940

CONCLUSION

A novel regional hydrophilic chip is developed for liquid dispensation. A droplets array is achieved by putting the chip surface in contact with reagents. The application of this chip is expanded by combining it with a gradient generator. High throughput toxicity screening of CdSe quantum dots is executed on the chip. CEA rapid detection on chip is realized via MBs-based sandwich immunoassay methods.

ASSOCIATED CONTENT

Supporting Information

Images of contact angles, fluorescence spectra, and fluorescence images of CdSe; DLS results of MBs. This material is available free of charge via the Internet at http://pubs.acs.org.

AUTHOR INFORMATION

Corresponding Author

*E-mail: xujj@nju.edu.cn.

Notes

The authors declare no competing financial interest.

ACKNOWLEDGMENTS

The authors are grateful for financial support from the 973 Program (Grants 2012CB932600, 2012CB933804) and the National Natural Science Foundation (Grants 21327902 and 21121091) of China.

REFERENCES

(1) Dittrich, P. S.; Manz, A. Lab-on-a-Chip: Microfluidics in Drug Discovery. *Nat. Rev. Drug Discovery* **2006**, *5*, 210−218.
(2) Bange, A.; Halsall, H. B.; Heineman, W. R. Microfluidic Immunosensor Systems. *Biosens. Bioelectron.* **2005**, *20*, 2488−2503.
(3) Tudos, A. J.; Besselink, G. A. J.; Schasfoort, R. B. M. Trends in Miniaturized Total Analysis Systems for Point-of-Care Testing in Clinical Chemistry. *Lab Chip* **2001**, *1*, 83−95.
(4) Fang, X.; Liu, Y.; Kong, J.; Jiang, X. Loop-Mediated Isothermal Amplification Integrated on Microfluidic Chips for Point-of-Care Quantitative Detection of Pathogens. *Anal. Chem.* **2010**, *82*, 3002−3006.
(5) Martinez, A. W.; Phillips, S. T.; Whitesides, G. M.; Carrilho, E. Diagnostics for the Developing World: Microfluidic Paper-Based Analytical Devices. *Anal. Chem.* **2010**, *82*, 3−10.
(6) Peeling, R. W.; Holmes, K. K.; Mabey, D.; Ronald, A. Rapid Tests for Sexually Transmitted Infections (STIs): The Way Forward. *Sex. Transm. Infect.* **2006**, *82*, v1−6.
(7) Lin, Z.; Ma, Y.; Zhao, C.; Chen, R.; Zhu, X.; Zhang, L.; Yan, X.; Yang, W. An Extremely Simple Method for Fabricating 3D Protein Microarrays with an Anti-Fouling Background and High Protein Capacity. *Lab Chip* **2014**, *14*, 2505−2514.
(8) Gutmann, O.; Kuehlewein, R.; Reinbold, S.; Niekrawietz, R.; Steinert, C. P.; de Heij, B.; Zengerle, R.; Daub, M. Fast and Reliable Protein Microarray Production by a New Drop-in-Drop Technique. *Lab Chip* **2005**, *5*, 675−681.
(9) Park, J. U.; Lee, S.; Unarunotai, S.; Sun, Y. G.; Dunham, S.; Song, T.; Ferreira, P. M.; Alleyene, A. G.; Paik, U.; Rogers, J. A. Nanoscale, Electrified Liquid Jets for High-Resolution Printing of Charge. *Nano Lett.* **2010**, *10*, 584−591.
(10) Liu, M. J.; Wang, J. X.; He, M.; Wang, L. B.; Li, F. Y.; Jiang, L.; Song, Y. L. Inkjet Printing Controllable Footprint Lines by Regulating the Dynamic Wettability of Coalescing Ink Droplets. *ACS Appl. Mater. Interfaces* **2014**, *6*, 13344−13348.
(11) Luo, Y. Q.; Yu, F.; Zare, R. N. Microfluidic Device for Immunoassays Based on Surface Plasmon Resonance Imaging. *Lab Chip* **2008**, *8*, 694−700.
(12) Mahendran, V.; Philip, J. Influence of Ag^+ Interaction on 1D Droplet Array Spacing and the Repulsive Forces between Stimuli-Responsive Nanoemulsion Droplets. *Langmuir* **2014**, *30*, 10213−10220.
(13) Sun, Y.; Zhou, X.; Yu, Y. A Novel Picoliter Droplet Array for Parallel Real-Time Polymerase Chain Reaction Based on Double-Inkjet Printing. *Lab Chip* **2014**, *14*, 3603−3610.
(14) Wang, C. H.; Lee, G. B. Automatic Bio-Sampling Chips Integrated with Micro-Pumps and Micro-Valves for Disease Detection. *Biosens. Bioelectron.* **2005**, *21*, 419−425.
(15) Xu, L.; Lee, H.; Oh, K. W. Syringe-Assisted Point-of-Care Micropumping Utilizing the Gas Permeability of Polydimethylsiloxane. *Microfluid. Nanofluid.* **2014**, *17*, 745−750.
(16) Hosokawa, K.; Omata, M.; Maeda, M. Immunoassay on a Power-Free Microchip with Laminar Flow-Assisted Dendritic Amplification. *Anal. Chem.* **2007**, *79*, 6000−6004.
(17) Yu, L.; Li, C. M.; Liu, Y.; Gao, J.; Wang, W.; Gan, Y. Flow-Through Functionalized PDMS Microfluidic Channels with Dextran Derivative for ELISAs. *Lab Chip* **2009**, *9*, 1243−1247.
(18) Cai, Q.; Tsai, C.; DeNatale, J.; Chen, C. L. Fluid Mixing in Micro-Scale Channel Patterned Hydrophobic/Hydrophilic Surface. *Micro-Electro-Mech. Syst.* **2007**, *8*, 27−31.
(19) Toma, M.; Loget, G.; Corn, R. M. Flexible Teflon Nanocone Array Surfaces with Tunable Superhydrophobicity for Self-Cleaning and Aqueous Droplet Patterning. *ACS Appl. Mater. Interfaces* **2014**, *6*, 11110−11117.
(20) Tullis, J.; Park, C. L.; Abbyad, P. Selective Fusion of Anchored Droplets via Changes in Surfactant Concentration. *Lab Chip* **2014**, *14*, 3285−3289.
(21) Neto, A. I.; Correia, C. R.; Custodio, C. A.; Mano, J. F. Biomimetic Miniaturized Platform Able to Sustain Arrays of Liquid Droplets for High-Throughput Combinatorial Tests. *Adv. Funct. Mater.* **2014**, *24*, 5096−5103.
(22) Tonooka, T.; Sato, K.; Osaki, T.; Kawano, R.; Takeuchi, S. Lipid Bilayers on a Picoliter Microdroplet Array for Rapid Fluorescence Detection of Membrane Transport. *Small* **2014**, *10*, 3275−3282.
(23) Wang, J. B.; Zhou, Y.; Qiu, H. W.; Huang, H.; Sun, C. H.; Xi, J. Z.; Huang, Y. Y. A Chip-to-Chip Nanoliter Microfluidic Dispenser. *Lab Chip* **2009**, *9*, 1831−1835.
(24) Xu, B. Y.; Yan, X. N.; Zhang, J. D.; Xu, J. J.; Chen, H. Y. Glass Etching to Bridge Micro- and Nanofluidics. *Lab Chip* **2012**, *12*, 381−386.
(25) Xu, B. Y.; Hu, S. W.; Qian, G. S.; Xu, J. J.; Chen, H. Y. A Novel Microfluidic Platform with Stable Concentration Gradient for on Chip Cell Culture and Screening Assays. *Lab Chip* **2013**, *13*, 3714−3720.
(26) Yu, X.; Xia, H. S.; Sun, Z. D.; Lin, Y.; Wang, K.; Yu, J.; Tang, H.; Pang, D. W.; Zhang, Z. L. On-Chip Dual Detection of Cancer Biomarkers directly in Serum Based on Self-Assembled Magnetic Bead Patterns and Quantum Dots. *Biosens. Bioelectron.* **2013**, *41*, 129−136.
(27) De Luca, A.; Depalo, N.; Fanizza, E.; Striccoli, M.; Curri, M. L.; Infusino, M.; Rashed, A. R.; La Deda, M.; Strangi, G. Plasmon Mediated Super-Absorber Flexible Nanocomposites for Metamaterials. *Nanoscale* **2013**, *5*, 6097−6105.
(28) Cebeci, F. C.; Wu, Z. Z.; Zhai, L.; Cohen, R. E.; Rubner, M. F. Nanoporosity-Driven Superhydrophilicity: A Means to Create Multifunctional Antifogging Coatings. *Langmuir* **2006**, *22*, 2856−2862.
(29) Jiang, Y. G.; Wang, Z. Q.; Yu, X.; Shi, F.; Xu, H. P.; Zhang, X.; Smet, M.; Dehaen, W. Self-Assembled Monolayers of Dendron Thiols for Electrodeposition of Gold Nanostructures: Toward Fabrication of Superhydrophobic/Superhydrophilic Surfaces and pH-Responsive Surfaces. *Langmuir* **2005**, *21*, 1986−1990.
(30) Sun, T. L.; Wang, G. J.; Feng, L.; Liu, B. Q.; Ma, Y. M.; Jiang, L.; Zhu, D. B. Reversible Switching between Superhydrophilicity and Superhydrophobicity. *Angew. Chem., Int. Ed.* **2004**, *43*, 357−360.
(31) Tu, Q.; Wang, J. C.; Zhang, Y. R.; Liu, R.; Liu, W. M.; Ren, L.; Shen, S. F.; Xu, J.; Zhao, L.; Wang, J. Y. Surface Modification of poly(dimethylsiloxane) and Its Applications in Microfluidics-Based Biological Analysis. *Rev. Anal. Chem.* **2012**, *31*, 177−192.

DOI: 10.1021/am5075216
ACS Appl. Mater. Interfaces 2015, 7, 935−940

(32) Marmur, A. The Lotus Effect: Superhydrophobicity and Metastability. *Langmuir* **2004**, *20*, 3517−3519.
(33) Hu, S. W.; Xu, B. Y.; Xu, J. J.; Chen, H. Y. Liquid Gradient in Two-Dimensional Matrix for High Throughput Screening. *Biomicrofluidics* **2013**, *7*, 064116.
(34) Rossier, J. S.; Gokulrangan, G.; Girault, H. H.; Svojanovsky, S.; Wilson, G. S. Characterization of Protein Adsorption and Immunosorption Kinetics in Photoablated Polymer Microchannels. *Langmuir* **2000**, *16*, 8489−8494.
(35) Liu, Y. J.; Guo, S. S.; Zhang, Z. L.; Huang, W. H.; Baigl, D. M.; Chen, Y.; Pang, D. W. Integration of Minisolenoids in Microfluidic Device for Magnetic Bead-Based Immunoassays. *J. Appl. Phys.* **2007**, *102*, 084911.

DOI: 10.1021/am5075216
ACS Appl. Mater. Interfaces 2015, 7, 935−940